Tellus (1991), *43A*, 106–127

An isentropic analysis of the wintertime vorticity exchange in relation to extratropical heat sources and sinks

By MARTIN P. HOERLING and DONALD R. JOHNSON, *University of Wisconsin-Madison, Space Science and Engineering Center, 1225 West Dayton Street, Madison, Wisconsin 53706, USA*

(Manuscript received 23 October 1989; in final form 11 October 1990)

ABSTRACT

The influence of heat sources and sinks on the time-averaged atmospheric circulation is studied through an isentropic analysis of the balance of dynamic vorticity. The property of isentropic dynamic vorticity, the vertical component of the curl of the momentum ($\boldsymbol{k} \cdot \nabla_\theta \times \rho J_\theta \boldsymbol{U}$), is based on Bjerknes' definition of circulation, his theorems and their application to problems of physical hydrodynamics including the general circulation of the earth's atmosphere. The diagnostics emphasize the three-dimensional exchange of dynamic vorticity occurring within migratory cyclone-scale waves of the Northern Hemisphere extratropics. Analysis reveals that the maintenance of the dynamic vorticity balance in the wintertime Northern Hemisphere is directly coupled to the three-dimensional distribution of heating and cooling. An isentropic mass circulation previously identified transports energy from extratropical oceanic heat sources to polar continental heat sinks. A corresponding systematic vorticity exchange occurs through air-mass exchange within mid-latitudes between continents and oceans. In the lowest isentropic layers, the balance of dynamic vorticity is maintained by absolute vorticity transport from anticyclonic circulations over Asia, North America and Greenland to cyclonic circulations over the North Pacific and Atlantic Oceans in concert with solenoidal sources and sinks within these regions. The scale of dynamic vorticity transport and solenoidal processes that occur within the isentropic mass circulation correspond with the scale of extratropical heat sources and sinks. As such, the commonality among the scales of the isentropic mass circulation, energy exchange and vorticity exchange reveals a direct response to differential heating in the maintenance of the time-averaged extratropical circulation of the Northern Hemisphere.

1. Introduction

By virtue of his interest in extratropical and tropical cyclones, Palmén (1951) emphasized the need to understand the systematic influence of migratory atmospheric disturbances on the general circulation. His analyses of the extratropical exchange of air masses including large-scale "slant-wise convection" were particularly revealing. This baroclinic exchange involves equatorward mass transport at lower potential temperatures and poleward mass transport at higher potential temperatures. The resulting isentropic mass circulation systematically transports energy from heat sources over mid-latitude oceans to heat sinks over polar continents and reveals a direct response to differential heating (Johnson et al., 1985; Townsend and Johnson, 1985).

An important problem is to understand how atmospheric circulation develops in response to heat sources and sinks. Sir Napier Shaw's (1930) discussion of the general circulaton stressed differences of entropy and its changes in order to illuminate the relation between differential heating and atmospheric motion. His synthesis of the general circulation included an underworld of polar air with lesser entropy and an overworld of subtropical air with greater entropy. The underworld was separated from the overworld by an entropy surface of intermediate value which sloped from the mid-troposphere of high latitudes to the earth's surface at the polar front.

From the point of view of isentropic vorticity exchange, Petterssen (1950, 1956) conceptualized the maintenance of the general circulation in relation to heat sources and sinks. His model of the

Northern Hemispheric wintertime circulation depicted a systematic transport of vorticity from its source regions over the Asian and North American continents to sink regions over the Pacific and Atlantic Oceans. In an isentropic analysis of dynamic vorticity for January 1979 presented herein, results will emphasize how differential heating and isentropic mass circulations combine to transport vorticity in a manner suggested by Petterssen.

Within the zonally averaged circulation, an exchange of angular momentum between frictional sources in the tropical easterlies and frictional sinks in mid-latitude westerlies is required to maintain steady zonal circulation. Correspondingly, an exchange of the curl of momentum (Kao, 1960), termed dynamic vorticity in this paper, is required between frictional sources in anticyclonic circulations and sinks in cyclonic circulations. Kao (1960) argued that the zonally averaged cyclonic circulation of polar and extratropical latitudes is maintained by a systematic transport of dynamic vorticity toward the pole by the perturbations in the westerlies. This exchange is essential for the maintenance of cyclonic vorticity poleward and anticyclonic vorticity equatorward of the mid-latitude westerlies. However, this exchange does not focus on the underlying processes that maintain the quasi-permanent zonally asymmetric circulations involved with the continents and oceans.

Important climatic features of the regional wintertime circulations are quasi-permanent cyclones over the North Pacific and Atlantic Oceans and anticyclones over Asia, North America and the subtropical oceans. In view of the influence of continents and oceans on energy balance, a complete understanding of the climatic response of circulation to differential heating requires consideration of the three-dimensional distribution of momentum and vorticity exchange.

The precedent dynamical study revealing the importance of heat sources and sinks on the planetary circulation was conducted by Smagorinsky (1953). This study has been followed by numerous other dynamical studies (e.g., Derome and Wiin Nielsen, 1971; Hoskins and Karoly, 1981; Held, 1983; Chen and Trenberth, 1988). Extensive isobaric observational studies which document the strong longitudinal and vertical variations of heat, momentum, and vorticity exchange of the wintertime circulation have also been presented (e.g., Blackmon et al., 1977; Lau 1978, 1979a, 1979b; Holopainen and Oort, 1981).

In a time-averaged isobaric vorticity analysis, Holopainen and Oort (1981) and Lau (1979a) demonstrate the transport of vorticity in the upper tropospheric westerlies which couples anticyclonic source regions over Asia and North America with cyclonic sink regions over the North Pacific and Atlantic. However, the structure of vorticity transport in the upper troposphere and its relation to systematic air mass exchange in the lower troposphere between heat source and heat sink regions remains ill defined apart from the characteristic state of quasi-geostrophic balance. Since this state of balance is maintained through transient secondary circulations, no direct link is established between the transport of energy and vorticity by a systematic mass circulation at a scale which is common with the scale of thermal forcing imposed.

Isentropic analyses of the mass, energy and angular momentum exchange in combination with estimates of the global distribution of heating have provided insight on global monsoonal circulations (Schaack, 1982; Johnson et al., 1985; Johnson, 1985a, b; Johnson, 1989). The physical basis for global monsoonal circulations with ascending branches through heat sources, descending branches through heat sinks and quasi-horizontal branches within isentropic layers coupling heat source and heat sink regions is discussed in detail by Johnson (1989). A basic aspect of global monsoonal circulations is that the concurrent transport of mass, energy and entropy constitutes a direct response to differential heating. From these isentropic results, a unique perspective of the response of the general circulation to planetary scale heating and cooling has emerged.

Knowledge of the isentropic structure of momentum and vorticity exchange in global monsoonal circulations in relation to differential heating, however, is still incomplete. In accord with Gallimore and Johnson's (1981) results, the scales of the isentropic Hadley circulation and the dynamical forcing by the total angular momentum torque are common (Townsend and Johnson, 1985; Johnson, 1985a). However, the varied nature of angular momentum exchange relative to mass and energy exchange makes the establishment of a direct link difficult.

Johnson and Hoerling (1988) (hereafter JH) set forth a diagnostic strategy to investigate the relation among dynamic vorticity balance, differential heating and the irrotational isentropic mass circulation. According to the analyses of Johnson et al. (1985) for January 1979, a thermodynamically coupled mass circulation is embedded in the polar-extratropical latitudes beneath 300 K which couples heat souces over the mid-latitude Pacific and Atlantic Oceans with heat sinks over the Asian and North American continents. This circulation in the underworld is also part of a global scale mass circulation above 300 K which couples heat sources over Indonesia, South America and Brazil with heat sinks over Africa, North America, Asia and the subtropical Pacific and Atlantic. On this global scale the thermally-forced mass circulation occurs through systematic air mass exchanges: in the underworld, polar air masses migrate from heat sinks at higher latitudes to heat sources at lower latitudes, while in the overworld subtropical and tropical air masses migrate from heat sources at lower latitudes to heat sinks at higher latitudes.

In view of these two distinct features of the wintertime isentropic mass circulation, the results that follow will focus on a regional-scale perspective of dynamic vorticity exchange. This exchange will be related to the distribution of continents and oceans, atmospheric heat sources and sinks and the thermally forced mass circulation in the underworld of the Northern Hemisphere extratropics. A global perspective of dynamic vorticity exchange in relation to planetary-scale heat sources and sinks is discussed by Hoerling (1987).

The insight on the maintenance of the rotational component of momentum provided differs from that presented in previous studies. In part, these differences stem from the choice of isentropic dynamic vorticity as opposed to kinematic vorticity as a descriptor of the circulation. Additionally, as discussed in JH, differences arise from the distinction in first-order balances of dynamic and kinematic vorticities as revealed in the relative magnitude of terms within isobaric and isentropic formulations. Thus, perspectives on the physical behaviour of the time-averaged circulation become coordinate dependent. The origin of this dependency is partly mathematical in the sense that the Eulerian representation of the non-linear exchange of properties in relation to Lagrangian processes is not unique between the two coordinate systems (Johnson, 1980). It is also partly physical in that a solenoidal source of circulation from the action of pressure stresses will induce changes in dynamic vorticity, not so in kinematic vorticity. The challenge is to gain understanding of the processes which force and maintain the planetary circulation and in so doing determine the geographical distribution of climate.

In Section 2, the property of dynamic vorticity and its time rate of change are discussed briefly. The isentropic data set employed for this analysis is described in Section 3. A detailed discussion of dynamic vorticity balance within the underworld of the Northern Hemisphere extratropics is provided in Section 4, while the summary and conclusion are given in Section 5.

2. Dynamic vorticity and its time rate of change

2.1. Definition of dynamic vorticity

Following Bjerknes (1937), the vertical component of relative dynamic vorticity in isentropic coordinates is defined by

$$Z_\theta = \boldsymbol{k} \cdot (\nabla_\theta \times \rho J_\theta \boldsymbol{U}), \tag{1}$$

where ρJ_θ equal to $-g^{-1}\partial p/\partial\theta$ is the mass per isentropic volume element (see Appendix for a complete list of symbols). The terminology "dynamic vorticity" is based upon Bjerknes' (1937) discussions of line integral theorems in which kinematic circulation is defined as the line integral of the velocity, $\oint \boldsymbol{U} \cdot \mathrm{d}\boldsymbol{r}$, while dynamic circulation is defined as the line integral of the momentum, $\oint \rho \boldsymbol{U} \cdot \mathrm{d}\boldsymbol{r}$. A detailed discussion of isentropic dynamic vorticity and its change appears in JH.

With an expansion and division by ρJ_θ, the relation between relative dynamic (per unit mass) and kinematic vorticities in isentropic coordinates is

$$z_\theta = Z_\theta/\rho J_\theta, \tag{2a}$$

$$= \zeta_\theta - (\nabla_\theta \rho J_\theta) \cdot (\boldsymbol{k} \times \boldsymbol{U})/\rho J_\theta, \tag{2b}$$

where the kinematic vorticity is given by

$$\zeta_\theta = \boldsymbol{k} \cdot (\nabla_\theta \times \boldsymbol{U}). \tag{3}$$

The second term is the scalar product of the gradient of mass with the vector $\boldsymbol{k} \times \boldsymbol{U}$. A relation with angular momentum is evident with the recognition that $\boldsymbol{k}\times\boldsymbol{U}$ corresponds with the moment of momentum per unit mass about the center of the earth divided by the length of the radius vector $\boldsymbol{r}$. In a barotropic hydrostatic atmosphere, dynamic vorticity equals kinematic vorticity. In a baroclinic atmosphere, the two differ. As stated by Kao (1960), "it is certainly a loss in generality to treat the atmosphere as a barotropic fluid and assign to it an average density in evaluating the volume integral of vorticity".

2.2. The time-averaged isentropic dynamic vorticity equation

The time-averaged steady state isentropic dynamic vorticity equation, derived by applying the operator $\boldsymbol{k}\cdot\nabla_\theta\times(\ )$ to the momentum transport equation (see JH for a detailed derivation), is expressed by

$$\overline{\nabla_\theta\cdot[\rho J_\theta \boldsymbol{U}(\zeta_\theta+f)]}=-\overline{\boldsymbol{k}\cdot(\nabla_\theta\times\rho J_\theta\nabla_\theta\psi)}+\overline{\boldsymbol{k}\cdot(\nabla_\theta\times\rho J_\theta \boldsymbol{F})}-\overline{\rho J_\theta\dot\theta\,\partial\zeta_\theta/\partial\theta}-\overline{\boldsymbol{k}\cdot(\nabla_\theta\rho J_\theta\dot\theta\times\partial\boldsymbol{U}/\partial\theta)}-\overline{\boldsymbol{k}\cdot(\nabla_\theta\times\rho J_\theta\nabla_\theta k)},\quad(4)$$

where the kinetic energy and the time average are defined by

$$k=(\boldsymbol{U}\cdot\boldsymbol{U})/2,\quad(5)$$

$$\bar h=\frac{1}{T}\int_{t_1}^{t_2}h\,\mathrm{d}t,\quad(6)$$

and terms involving the mass tendency have been assumed small. The right-hand terms of (4) are the mass-dry static energy solenoidal source as defined by the curl of the pressure gradient force, the curl of the friction force, vertical advection of relative vorticity, tilting of vortex tubes by the diabatic mass flux, and a mass-kinetic energy solenoidal source. Maintenance of a steady state for isentropic dynamic vorticity in the presence of an imbalance of processes on the right side of (4) requires the absolute vorticity transport to be divergent.

A key difference between the balances of dynamic and kinematic isentropic vorticities involves mass-dry static energy solenoids of a baroclinic atmosphere. With the application of a vector identity and substitution of the geostrophic wind relation, the mass-dry static energy solenoidal source is expressed by

$$-\boldsymbol{k}\cdot(\nabla_\theta\times\rho J_\theta\nabla_\theta\psi)=\boldsymbol{k}\cdot[\nabla_\theta\rho J_\theta\times(-\nabla_\theta\psi)],\quad(7a)$$

$$=f\boldsymbol{U}_g\cdot\nabla_\theta\rho J_\theta.\quad(7b)$$

The schematic in Fig. 1 shows an intersection of isopleths of mass and dry static energy. A positive solenoidal field is depicted with cyclonic acceleration from the condition that the vector product $\nabla_\theta\rho J_\theta\times(-\nabla_\theta\psi)$ is directed along $\boldsymbol{k}$. In the form of (7b) the solenoidal acceleration is equivalent to the geostrophic advection of mass. In Fig. 1 the scalar product of $\boldsymbol{U}_g$ and $\nabla_\theta\rho J_\theta$ is positive revealing that the solenoidal source of dynamic vorticity is associated with a negative geostrophic advection of mass.

The area integral of the source of dynamic vorticity may be interpreted in terms of the acceleration of dynamic circulation along curve Q in Fig. 1. The cyclonic acceleration by the mass weighted pressure gradient force $(-\rho J_\theta\nabla_\theta\psi)$ along the segment of the path of integration (Q) directed towards lower dry static energy is greater in magnitude than the anticyclonic acceleration along the segment directed towards higher dry static energy. The resulting net cyclonic acceleration stems from the greater mass within the isentropic layer along the segment of Q directed

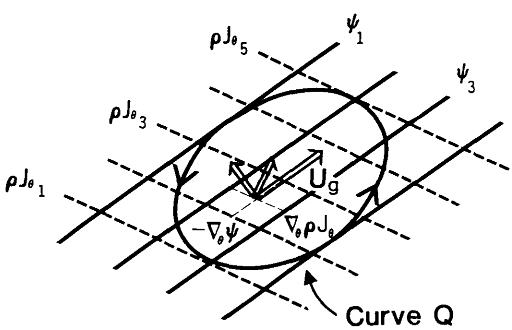

Fig. 1. Schematic of the acceleration of circulation by mass-dry static energy solenoids enclosed by the curve Q. Dashed isopleths indicate mass labeled as ρJ_θ and solid isopleths the dry static energy (Montgomery Stream Function) labeled as ψ. The gradients of mass, dry static energy and the geostrophic velocity indicated by vectors portray the negative geostrophic advection of mass that is synonymous with a positive solenoidal source of dynamic vorticity.

towards lower dry static energy than in the segment directed towards higher dry static energy.

As discussed in JH, this solenoidal source of dynamic vorticity occurs in baroclinic disturbances through the transfer of momentum across inclined isentropic surfaces by pressure stresses. The sense of the transfer is directed from isentropic layers with negative solenoids to layers with positive solenoinds. This process is a key component of the first-order balance of the rotational component of the isentropic mass transport and is a fundamental process linking thermo- and hydrodynamics (Bjerknes, 1937).

3. Data set and analysis methods

The Global Weather Experiment (GWE) data set employed for the present study is the European Centre for Medium Range Weather Forecasts (ECMWF) Level IIIb main analyses for January 1979. The isobaric to isentropic conversion was based upon the assumption that pressure and other basic meteorological variables vary linearly with the R/c_p power of pressure. The vertical profile of temperature is adjusted to remove any superadiabatic lapse rates. The resulting isentropic data with a vertical resolution of 10 K extending from 240 K to 380 K consisted of 16 isentropic layers. The latitudinal-longitudinal resolution used in the analysis was 3.75° with u, v, T, z, RH and p defined at each grid point. The Montgomery stream function and mass were subsequently computed following Townsend and Johnson (1985).

3.1. Numerical methods

All terms of the dynamic vorticity equation were temporally averaged for each 10 K isentropic layer from 0000 and 1200 UTC data during the month of January 1979. The Lorenz convention that underground isentropic surfaces are contiguous with the earth's surface was used (Townsend and Johnson, 1985). Since ρJ_θ vanishes in underground isentropic surfaces, a process or property in such layers is identically zero.

For each time period, an adjustment is made to the horizontal mass divergence at each grid point to ensure that the vertically integrated mass continuity equation used to estimate the diabatic mass flux is satisfied (Wei et al., 1983). The adjusted horizontal mass divergence is used in the computation of divergence terms, the diabatic mass flux and the irrotational component of isentropic mass transport. The Poisson equation used to relate the irrotational component of the mass transport with the horizontal divergence of the mass transport (Johnson, et al., 1985) is given by

$$\nabla_\theta^2 \bar{X}_\rho = \nabla_\theta \cdot (\overline{\rho J_\theta \mathbf{U}}) = \delta. \tag{8}$$

Eq. (8) is solved on the global spherical grid with period boundary conditions using the Buneman variant of cyclic reduction (Swarztrauber and Sweet, 1975).

For the analyses presented, zonal and meridional filtering is applied to the final computations which preserves the large-scale structure while effectively damping small-scale structure. A one-dimensional zonal Fourier filter truncates harmonics having wavelengths less than 4000 km. Four passes of a low pass filter having weights (2, 3, 2) and one pass of an inverse filter having weights (-1, 5, -1) are applied meridionally. The frequency response for this combination of filtering is presented in Table 1 of Johnson et al., (1987).

4. Maintenance of the northern hemisphere dynamic vorticity balance during January 1979

4.1. *An isentropic analysis of the northern hemisphere circulation*

4.1.1. Synoptic overview. The dominant features of the mean sea level circulation for January 1979 in Fig. 2a are the Siberian high and the Aleutian low. In contrast, the wintertime low pressure near Iceland is disorganized with three weak troughs located near Newfoundland, Scandanavia and Spain. The subtropical highs of the Atlantic and Pacific Oceans are ill-defined within a zonal belt of high pressure extending along 30° N.

Although the Icelandic low is poorly defined in the monthly mean surface pressure field, the distribution of cyclone frequency during January 1979 (Fig. 2b) indicates a well-organized cyclone track stretching from the central United States to Newfoundland. The extension of this track northeastward toward Greenland is curtailed by blocking in the North Atlantic. In association with this blocking, the climatologically favored region

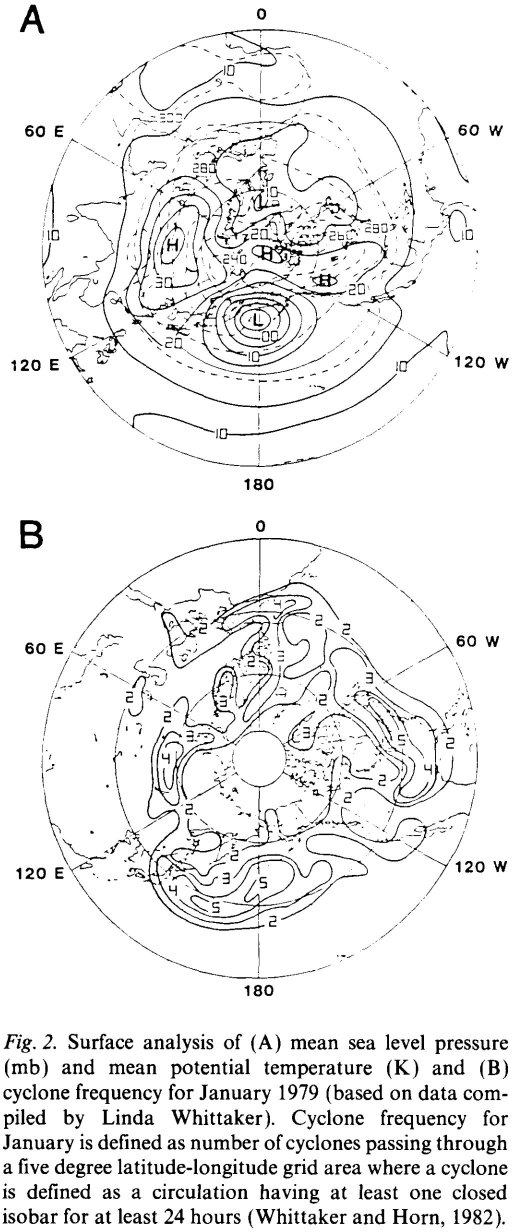

Fig. 2. Surface analysis of (A) mean sea level pressure (mb) and mean potential temperature (K) and (B) cyclone frequency for January 1979 (based on data compiled by Linda Whittaker). Cyclone frequency for January is defined as number of cyclones passing through a five degree latitude-longitude grid area where a cyclone is defined as a circulation having at least one closed isobar for at least 24 hours (Whittaker and Horn, 1982).

of cyclogenesis along the Atlantic seaboard is shifted westward across the eastern United States. The major Pacific cyclone track stretching from Japan to the Aleutians is active throughout the month. Other cyclone tracks are evident across the Mediterranean Sea and Siberia, and to the east of Iceland.

The distributions of pressure, Montgomery Stream Function and mass for the 260–270 K and 280–290 K isentropic layers within the underworld (defined herein as the domain confined beneath the 300 K surface) are illustrated in Figs. 3 and 4. The 260–270 K layer (Fig. 3a) slopes from the earth's surface in mid-latitudes to near 700 mb in polar latitudes. Regions of enhanced slope occur along the coasts of Asia, North America and Greenland in association with the stronger baroclinity located between continental and maritime air masses. The 280–290 K layer (Fig. 3b) extends from the earth's surface in subtropical latitudes to nearly 400 mb across Siberia and 500 mb across northeastern Canada.

The monthly layer-averaged Montgomery Stream Function and monthly-averaged mass distribution for the 260–270 K and the 280–290 K layers are presented in Figs. 4a and b, respectively. The zero contour for mass designates the equatorward limit of the given isentropic layer during January. The prominent features in the 260–270 K layer are the two closed cyclonic circulations with centers located near the western Aleutian Islands and Hudson Bay. Strong northwesterly flow is evident across Asia and the western Pacific, while weaker northwesterly flow extends across north central Canada eastward. This flow is associated with mean positive geostrophic advection of mass across the western Pacific and Atlantic Oceans (Fig. 4a). Prominent features of the mid-tropospheric circulation in the 280–290 K layer (Fig. 4b) are the Asian and North American jet streams, a North American trough with southwest-northeast tilt and a diffluent Asian trough with southeast-northwest tilt. Downstream of the mean troughs are mean ridges with axes centered along 130° W and 30° W.

4.1.2. Dynamic vorticity. The distributions of dynamic vorticity for the 260–270 K and 280–290 K layers are presented in Figs. 5a and b, respectively. Cyclonic dynamic vorticity extends across northern Asia, the North Pacific and eastern North America, while anticyclonic dynamic vorticity extends across polar regions of the continents and the mid-latitudes of the Pacific. Centers of maximum cyclonic dynamic vorticity coincide with the mean troughs over Asia, the western Pacific and North America. A maximum of anticyclonic dynamic vorticity in high latitudes coincides with the mean ridge located over Alaska.

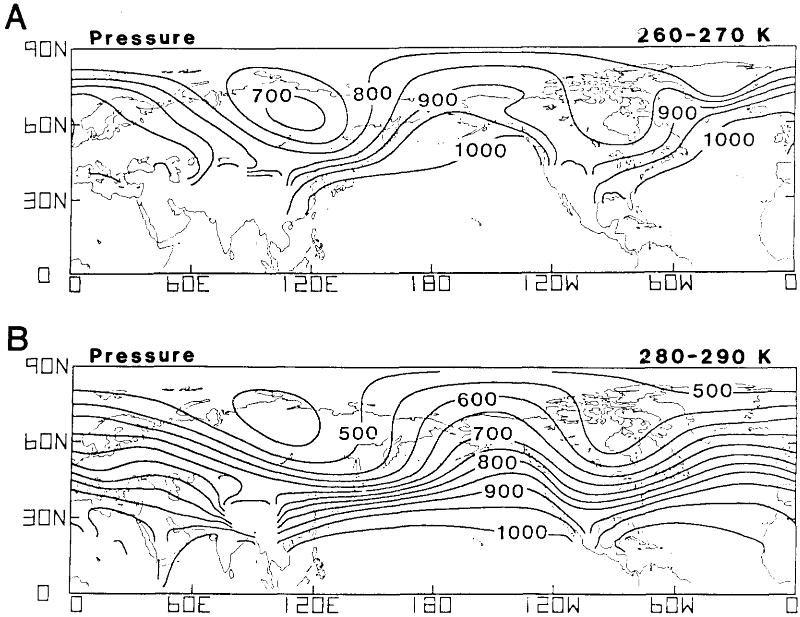

Fig. 3. Mean layer-averaged pressure (mb) for the (A) 260–270 K and (B) 280–290 K isentropic layers for January 1979.

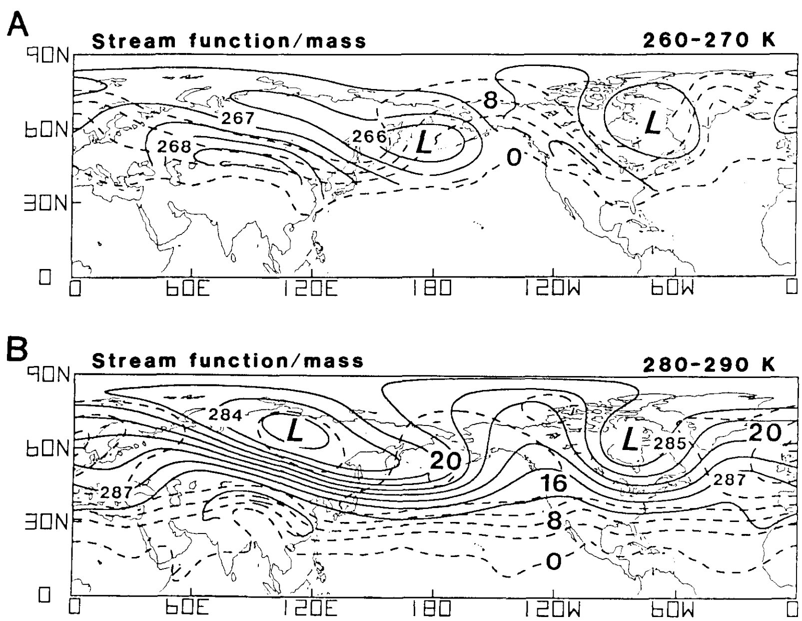

Fig. 4. Mean layer-averaged Montgomery Stream Function (solid contours) and mean layer-integrated mass (dashed contours) for the (A) 260–270 K and (B) 280–290 K isentropic layers (units, $10^3\ m^2\ s^{-2}$ and $10^2\ kg\ m^{-2}$, respectively) for January, 1979.

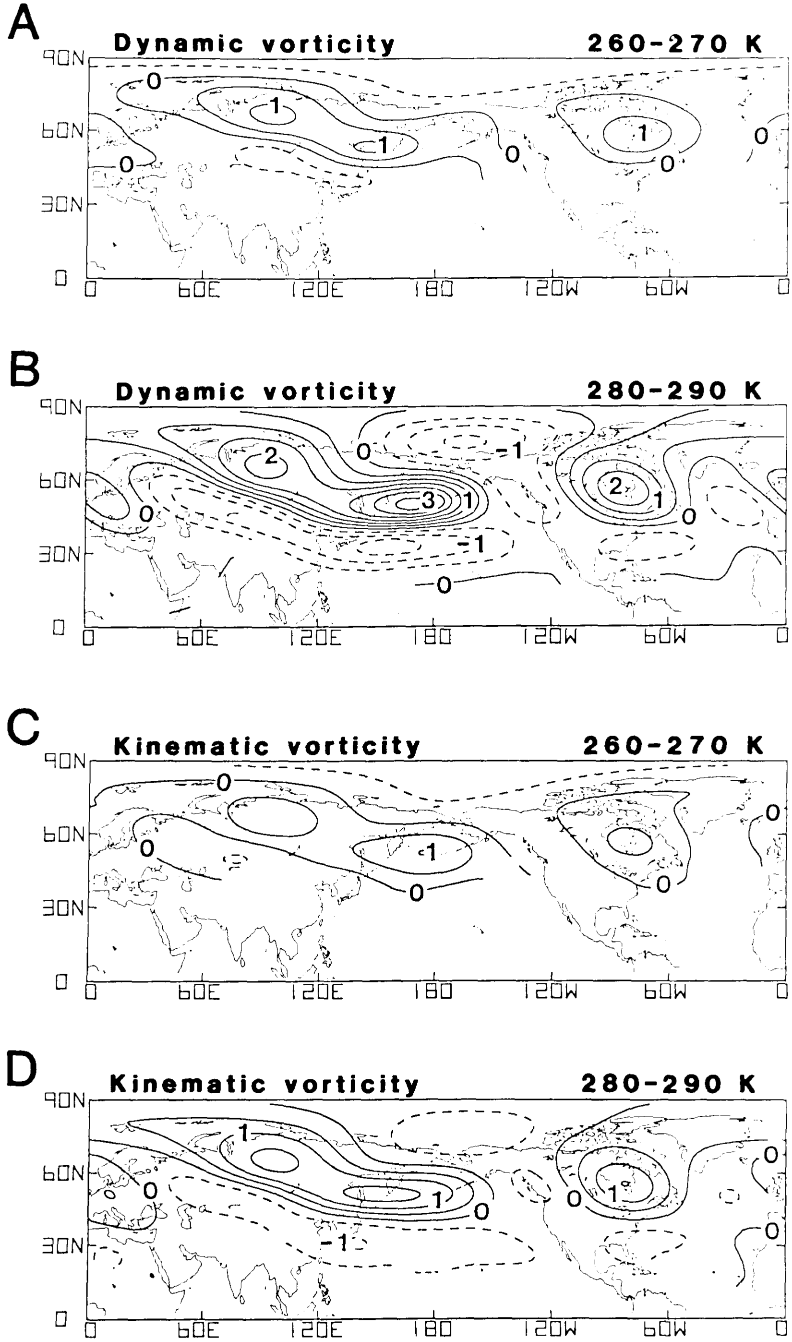

Fig. 5. Mean layer-integrated dynamic vorticity for the (A) 260–270 K and (B) 280–290 K isentropic layers (units, 10^{-2} kg m^{-2} s^{-1}) and mean layer-averaged relative vorticity for the (C) 260–270 K and (D) 280–290 K isentropic layers (units, 10^{-5} s^{-1}) for January 1979. Fields have been filtered to emphasize contributions from wavelengths greater than 4000 km.

Other anticyclonic centers downstream of Japan and the United States are associated with the anticyclonic shear of the westerlies.

Comparison with the mean kinematic vorticity distributions in the 260–270 K and 280–290 K layers (Figs. 5c and d) reveals that generally regions of cyclonic (anticyclonic) dynamic vorticity coincide with regions of cyclonic (anticyclonic) kinematic vorticity. However, some differences are evident. For example, the center of maximum cyclonic dynamic vorticity in the 260–270 K layer (Fig. 5a) is located near the Kamchatka Peninsula, while the maximum cyclonic kinematic vorticity is located downstream near the Aleutian Islands. The large gradient of mass within this intense baroclinic structure of the lower troposphere which separates the continental and oceanic regions largely accounts for the differences in the distributions of kinematic and dynamic vorticities.

4.2. Thermally forced mass circulations in the underworld

An overview of the thermally forced mass circulation in the underworld provides a point of departure for illustrating the relation between differential heating and dynamic vorticity balance. The distribution of heating averaged for the surface-290 K layer is reproduced from the analysis of Schaack and Johnson (1989) in Fig. 6a. The large-scale pattern reveals cooling across much of Asia and North America, while heating occurs over the Pacific and Atlantic Oceans. Heating over the oceans stems from the strong sensible and latent energy exchange as continental polar air masses move eastward over the Kuroshio, Gulf Stream and North Atlantic currents. Mean cooling within persistent anticyclonic circulations over Asia and North America results from the net infrared emission and the high albedo of extensive snow and ice cover.

In the time-averaged state, the irrotational component of isentropic mass transport is coupled to the distribution of heat sources and sinks (Johnson et al., 1985; Townsend and Johnson, 1985). In regions of upward (downward) diabatic mass flux, horizontal convergence (divergence) in lower-valued isentropic layers occurs in conjunction with divergence (convergence) in higher-valued layers. Through these processes, the planetary scales of horizontal mass transport and differential heating correspond, thereby establishing the thermally coupled nature of global monsoonal circulations.

The potential functions and the irrotational components of time-averaged mass transport for 260–270 K and 280–290 K layers (Johnson et al., 1985) appear in panels 6b and c, respectively. An outstanding feature of the irrotational mass circulation in the underworld during January is the systematic horizontal exchange of mass occurring between heat sink regions over Asia, North America and Greenland and heat source regions over the western Pacific and Atlantic Oceans. In the 260–270 K layer (Fig. 6b), the irrotational mass transport is directed from the continental heat sink regions to the oceanic heat source regions over the Kuroshio Current and Gulf Stream. The maximum transport of mass coincides with the isopleth of zero mass divergence that separates regions of mass divergence over the continents from mass convergence over the oceans. In the time-averaged state, this maximum also coincides with the boundary between heating and cooling. Note the transport is maximized along the east coasts of Asia and North America where the gradient of heating is maximized. Regions of strong mass convergence occur east of Japan and Newfoundland, and southeast of Greenland near the primary heat sources of the underworld. Similarly, regions of mass divergence occur over the polar latitudes of Asia and North America near the primary heat sinks of the underworld.

Within this two-layered structure, the sense of the mass transport in the 280–290 K layer (Fig. 6c) is reversed from the transport in the 260–270 K layer. Mass divergence occurring along the oceanic cyclone tracks in the 280–290 K layer is linked through mass continuity and compensation with lower layer mass convergence. Although less intense, mass convergence occurring over interior portions of Asia and North America in the 280–290 K layer is likewise linked with lower layer mass divergence. Associated with this distribution of the isentropic mass divergence in the 280–290 K layer is an irrotational component of mass transport from heat source regions along the Pacific and Atlantic storm tracks to the heat sink regions over the mean anticyclones of Asia and North America. The equatorward irrotational component of mass transport from mid-latitude to subtropical oceans in the 280–290 K layer stems from the upward diabatic mass flux to higher potential temperatures

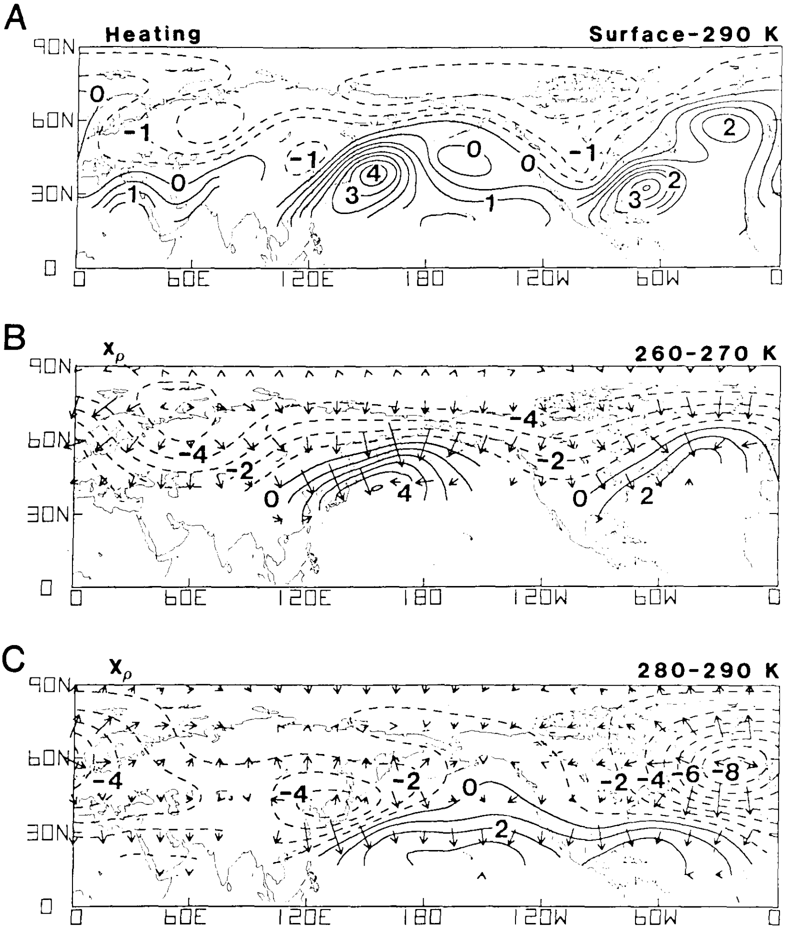

Fig. 6. (A) Mean surface-290 K mass-weighted averaged heating (K day^{-1}) and mean layer-integrated mass transport potential (X_ρ) and irrotational component of mass transport vectors for (B) 260–270 K isentropic layers (units, 10^9 kg s^{-1}) for January 1979. The field in panel A has filtered to emphasize contributions from wavelengths greater than 4000 km.

as polar air masses move equatorward and modify through sensible and latent heating during the amplification of baroclinic waves.

4.3. Dynamic vorticity balance within the underworld

Within the exchange of continental and maritime polar air masses, the monthly-averaged dynamic vorticity in the two-layered structure of the underworld during January is maintained primarily by a balance between the divergence of absolute vorticity transport (to be subsequently referred to as vorticity divergence) and mass-dry static energy solenoids

$$\nabla_\theta \cdot [\rho J_\theta \boldsymbol{U}(\zeta_\theta + f)] \simeq -\boldsymbol{k} \cdot (\nabla_\theta \times \rho J_\theta \nabla_\theta \psi). \qquad (9)$$

All of the remaining terms of the isentropic dynamic vorticity balance below 300 K as diagnosed for January 1979 were one order of magnitude less than the magnitude of the fields expressed in (9) (Hoerling, 1987). As such, only the results for the balance in (9) will be presented in this paper.

The contrast in the first-order balance of isentropic dynamic vorticity, as expressed by (9), with the balance for isobaric kinematic vorticity is interesting. The first order isobaric kinematic vorticity balance in the lower troposphere of extratropics occurs between vorticity divergence and source/sinks by friction (e.g., Holopainen and Oort, 1981; Mullen, 1986). In isentropic dynamic vorticity balance, friction is of second-order importance, while mass-dry static energy solenoids and the vorticity divergence are of first-order importance in the Northern Hemisphere extratropics. As implied by the geostrophic relation in (7b), solenoidal processes are also directly linked with the vorticity divergence since apart from the variation of the Coriolis parameter the geostrophic advection of mass is equal to the divergence of the geostrophic mass transport. Thus, solenoids play a primary role in maintaining the circulation of the underworld. The relations of solenoidal sources with heat sources and sinks is discussed in the next section, after which the relation of absolute vorticity transport to thermally coupled mass transport is presented.

4.3.1. The 260–270 K isentropic layer

(a) *Mass-dry static energy solenoids*

The distribution of mass-dry static energy solenoids for the 260–270 K layer is shown in Fig. 7a. Sinks of dynamic vorticity by negative solenoids (dashed contours) occur primarily across the North Pacific and Atlantic Oceans with centers located east of Japan and southwest of Iceland. These sinks are located within the strong low-level baroclinic zones separating continental from maritime polar air masses. The centers are coincident with positive geostrophic mass advection (see Fig. 4a) as the continental polar air masses migrate toward the mid-latitude of the Pacific and Atlantic Oceans in association with the eastward propagation of amplifying baroclinic disturbances. From a time-averaged perspective of the planetary-scale circulation, the net sink of dynamic vorticity occurring in these regions is determined by baroclinic processes occurring within propagating disturbances. Note the correspondence between axes of negative solenoids extending downstream of Asia and North America and the tracks of oceanic cyclones during January in Figs. 2b and 7a.

The source regions by positive solenoids which occur across northern Europe, northern Asia, Alaska, Canada and much of Greenland correspond primarily with mean anticyclonic circulations of the lower troposphere. Distinct centers are found over Finland, northern Alaska and Hudson Bay. For the 260–270 K layer as a whole, the zero isopleth separates positive solenoids in predominately polar latitudes from negative solenoids in middle latitudes.

A relationship between source/sinks of dynamic vorticity and of energy is suggested by the commonality in scales of the solenoid and diabatic heating distributions. In the 260–270 K layer, the two large-scale sink regions of dynamic vorticity across the North Pacific and North Atlantic coincide with the primary heat source regions of the underworld (see Fig. 6a). Similarly, three large-scale source regions of dynamic vorticity centered across western Asia, the Bering Sea and Hudson Bay coincide with the primary heat sink regions of the underworld.

(b) *Vorticity divergence*

In Fig. 7b, the time-averaged vorticity divergence (dashed contours) extends across northern Europe, northern Asia, Canada and much of Greeland. Centers of vorticity divergence occur west of the Urals and from the northern Soviet Union to northern Alaska. Vorticity convergence (solid contours) occurs across central Asia and the North Pacific and Atlantic Oceans with centers located east of Japan and southwest of Iceland. The primary process balancing the solenoidal source of dynamic vorticity in the 260–270 K layer (Fig. 7a) is the vorticity divergence (Fig. 7b). Along the oceanic storm tracks, the increase of dynamic vorticity by convergence of absolute vorticity transport balances sinks by solenoidal processes. In anticyclonic circulations of polar regions the decrease by vorticity divergence balances solenoidal sources.

The distribution of the mean irrotational component of absolute vorticity transport (defined as in (8) except $\rho J_\theta \vec{U}$ is replaced by $\rho J_\theta \vec{U}(\zeta_\theta + f)$) in the 260–270 K layer is presented in Fig. 7c. The irrotational component of vorticity transport is primarily directed from heat sinks over continents to heat sources over mid-latitude oceans. In the Eastern Hemisphere, maximum transport occurs over the Sea of Japan and northeastward along the

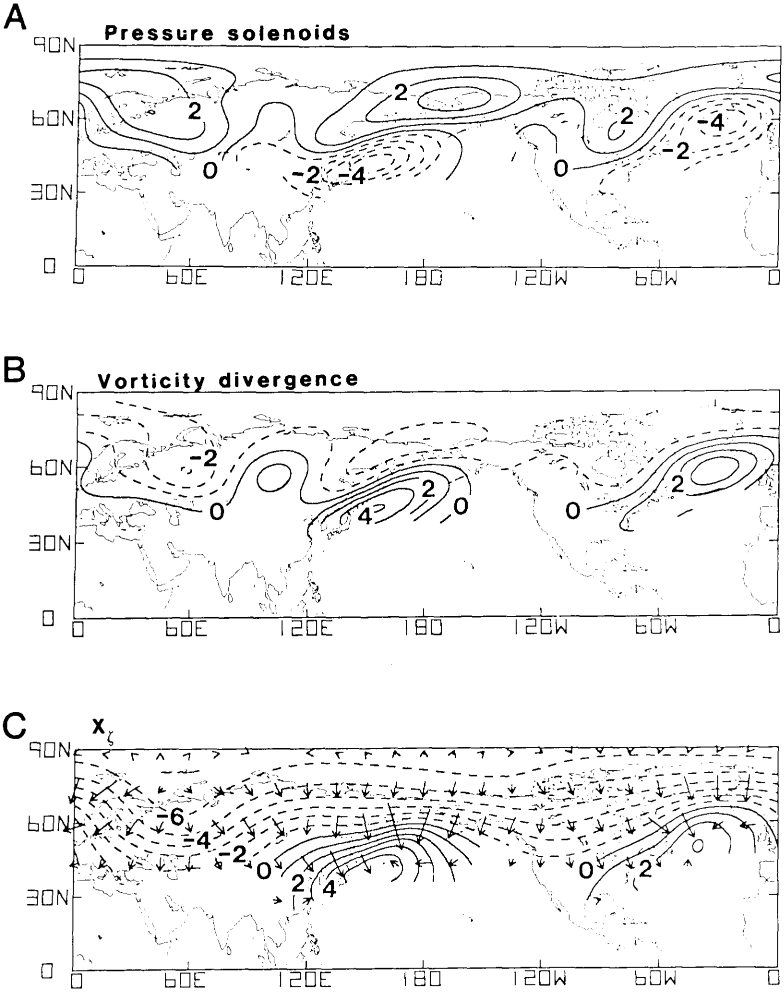

Fig. 7. Mean layer-integrated (A) mass-dry static energy solenoids and (B) vorticity divergence for the 260–270 K isentropic layer (units, 10^{-7} kg m^{-2} s^{-2}) and mean layer-integrated (C) absolute vorticity transport potential (X_ζ) (units, 10^5 kg s^{-2}) and irrotational component of absolute vorticity transport vector for January 1979. Fields in (A) and (B) have been filtered to emphasize contributions greater than 4000 km.

Soviet Union coastline to the Aleutians. In the Western Hemisphere, maximum transport occurs over eastern Canada and southern Greenland. A comparison of Figs. 6b and 7c reveals the similar distributions and horizontal scales of irrotational modes of absolute vorticity and mass transport. Since the latter scale corresponds with the scale of energy transport (Johnson et al., 1985; Johnson, 1989), all three scales become equivalent. Thus, the local vorticity source through convergence over the heat source regions of the Kuroshio, Gulf Stream and North Atlantic currents and the local vorticity sink through divergence over the heat sink regions of Asia, North America and Greenland are strongly coupled with the irrotational component of the mean isentropic mass circulation.

Further insight between thermally forced mass and vorticity transport is gained from the relationship between the divergent and advective com-

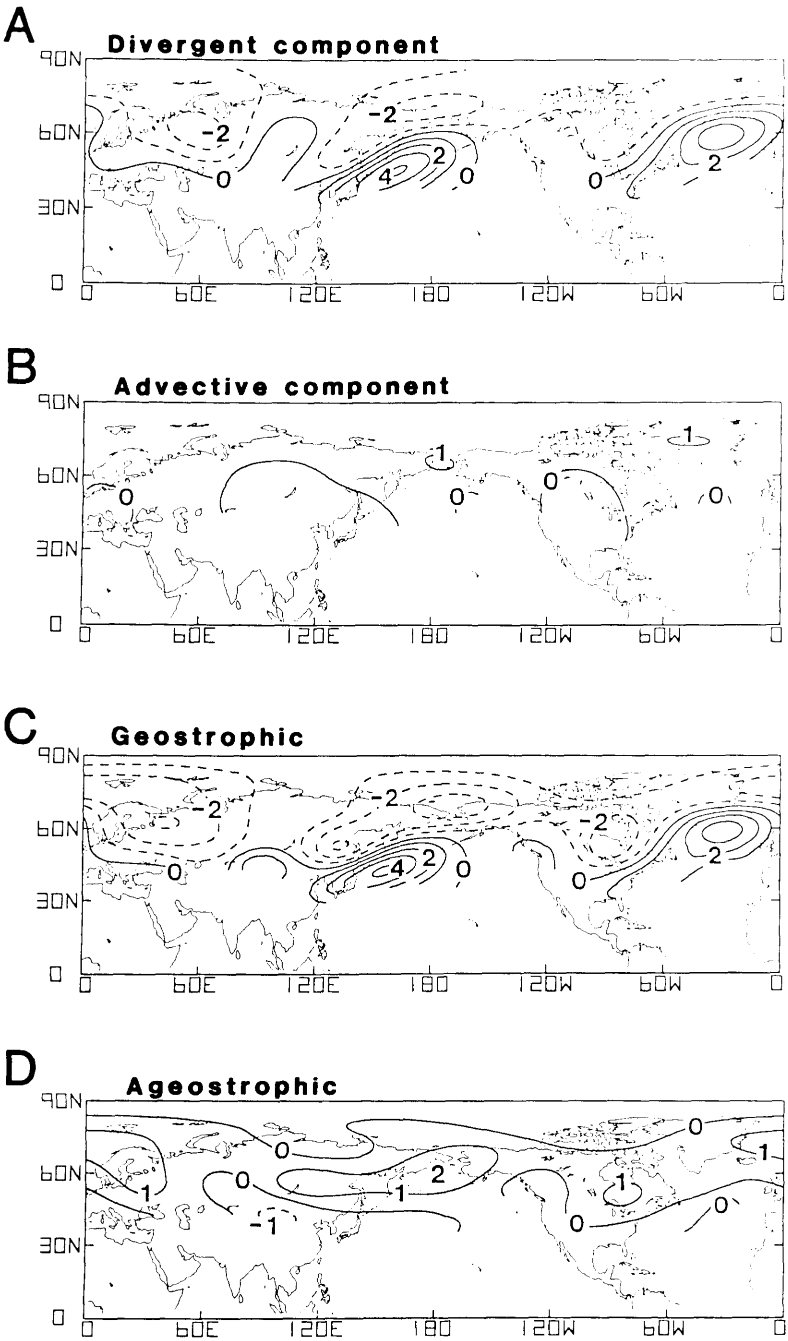

Fig. 8. Mean layer-integrated contributions of (A) mass divergence component and (B) horizontal advection component to the vorticity divergence shown in Fig. 7B along with the (C) geostrophic mode and (D) ageostrophic mode of the mass divergence component shown in (A) for 260–270 K isentropic layer (units, 10^{-7} kg m^{-2} s^{-2}) for January 1979. All fields have been filtered to emphasize contributions from wavelengths greater than 4000 km.

ponents of the time-averaged vorticity divergence given by

$$\overline{\nabla_\theta \cdot [\rho J_\theta \boldsymbol{U}(\zeta_\theta + f)]} = \overline{(\zeta_\theta + f)\, \nabla_\theta \cdot (\rho J_\theta \boldsymbol{U})} + \overline{\rho J_\theta \boldsymbol{U} \cdot \nabla_\theta (\zeta_\theta + f)}. \tag{10}$$

A comparison of the distributions of these two components, shown in Figs. 8a and b, with Fig. 7b reveals the distribution of the time-averaged vorticity divergence in the underworld to be determined primarily by the divergent component. This result is analogous with Mullen's (1986) results from an analysis of the lower tropospheric balance of kinematic vorticity across the North Pacific and Atlantic Oceans. During January, the generation of dynamic vorticity by mass convergence across the North Pacific and Atlantic occurs through stretching of vortex tubes. In low layers this systematic mass convergence along the storm tracks occurs during baroclinic development of extratropical cyclones (Johnson and Downey, 1976; Johnson and Hill, 1987). Similarly, local dynamic vorticity destruction occurs through mass divergence and shrinking of vortex tubes in anticyclonic vortices (Downey and Johnson, 1978; Lenzen, 1980) across western and eastern Asia, Canada and Greenland.

Through isentropic analysis, Johnson (1985a and b; 1989) also showed that the time-averaged energy balance of extratropical latitudes is maintained primarily through the transport of energy

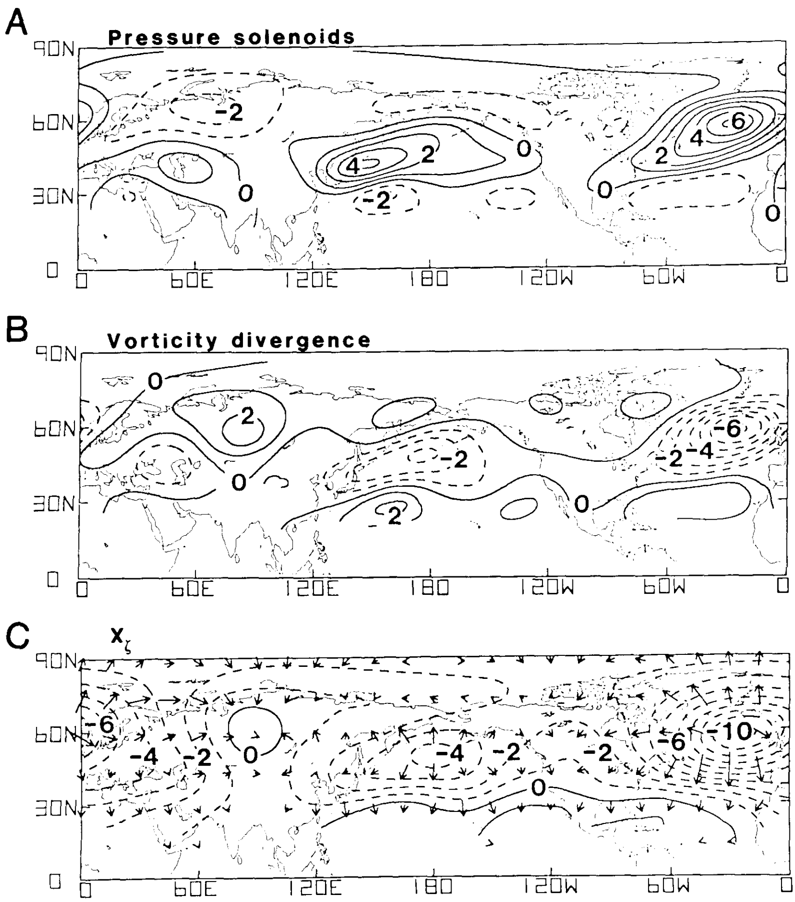

Fig. 9. Same as Fig. 7 except for the 280–290 K isentropic layer.

from heat sources to heat sinks by the time-averaged geostrophic isentropic mass circulation. The fundamental nature of the direct link of the thermally forced geostrophic transport of mass and energy with dynamic vorticity exchange is discussed in JH. The link between dynamic vorticity balance and the distribution of heat sources and sinks stems from the geostrophic nature of the isentropic mass divergence, energy divergence and solenoidal processes in mid-latitudes. In order to establish this behavior, the mass divergence component of (10) is expressed by

$$-\overline{(\zeta_\theta+f)\,\nabla_\theta\cdot(\rho J_\theta \boldsymbol{U})} = -\overline{(\zeta_\theta+f)\,\nabla_\theta\cdot(\rho J_\theta \boldsymbol{U}_{\mathrm{g}})} - \overline{(\zeta_\theta+f)\,\nabla_\theta\cdot(\rho J_\theta \boldsymbol{U}_{\mathrm{ag}})}, \qquad (11)$$

where $\boldsymbol{U}_{\mathrm{g}}$ and $\boldsymbol{U}_{\mathrm{ag}}$ are the geostrophic and ageostrophic velocities, respectively. Inspection of the geostrophic and ageostrophic contributions (Figs. 8c and d) reveals the dominance of the local source of dynamic vorticity in the underworld by the geostrophic mode of mass divergence. Likewise, comparison of Figs. 7b and 8c shows that the geostrophic mode of mass divergence is the primary component of the mean vorticity divergence in the 260–270 K layer. Thus, in extratropics the vorticity source from stretching within the lateral branches of the monsoonal circulation is realized primarily through the convergence of the geostrophic transport of absolute vorticity which largely balances mass-dry static energy solenoids. This compensation within the isentropic balance of dynamic vorticity is a reflection of the atmosphere's quasi-geostrophic balance.

4.3.2. The 280–290 K isentropic layer

(a) *Mass-dry static energy solenoids*

The selenoid distributions of the 280–290 K (Fig. 9a) and the 260–270 K layers are largely opposite. Outstanding features are the strong sources of dynamic vorticity occurring in the regions of intense baroclinic activity downstream of Asia, North America and Greenland. For the Northern Hemisphere as a whole, three large-scale solenoidal source regions with centers east of Japan, southwest of Iceland and over the Caspian Sea coincide with the primary surface cyclone tracks during January. The characteristic zonal scale of the mass-dry static energy solenoids in the 280–290 K layer of the extratropics is also that of continents and oceans.

Flanking the mid-latitude sources are sinks across subtropical latitudes and portions of polar latitudes. Three centers of solenoidal sinks occur near the Urals, the Bering Sea and Hudson Bay. Sinks of dynamic vorticity in the subtropics are most pronounced over the subtropical Atlantic and Pacific Oceans.

Isentropic vertical cross sections in Figs. 10a and 11a oriented along the Pacific and Atlantic storm tracks portray the vertical distributions of the mass-dry static energy solenoids, vorticity divergence and the diabatic mass flux $\rho J_\theta \dot{\theta}$. The cross sections in Fig. 10 extend along 43° N from central Manchuria at 120° E, across northern Japan at 150° E to south of the Gulf of Alaska at 150° W. The cross sections in Fig. 11 extend southwest-to-northeast from the southern United States at 30° N and 90° W, across the North Atlantic to north of the British Isles at 60° N and 0°. The importance of cyclone-scale processes in the underworld relative to the overworld in these regions is evident from the large magnitudes of the various processes below 300 K and the much smaller magnitudes above. Negative solenoids beneath the 280 K surface occur in association with the equatorward and eastward geostrophic advection of continental polar and arctic air masses as baroclinic disturbances propagate from Asia and North America to the north central Pacific and Atlantic. Positive solenoids above the 280 K surface occur in association with the poleward geostrophic advection of maritime polar air masses which originate over the Pacific and Atlantic.

The vertical reversal in sign of the solenoids across the storm tracks reveals a preferred mode of dynamic vorticity and angular momentum exchange between lateral branches of the mass circulation in developing cyclones. The condition that the area integral of dynamic vorticity is equal to dynamic circulation (JH), which when multiplied by a radial dimension equals angular momentum imposes a constraint that changes in dynamic vorticity and angular momentum are coupled. In particular, the areal integral of mass-dry static energy solenoids being a source of dynamic circulation is directly related to sources of

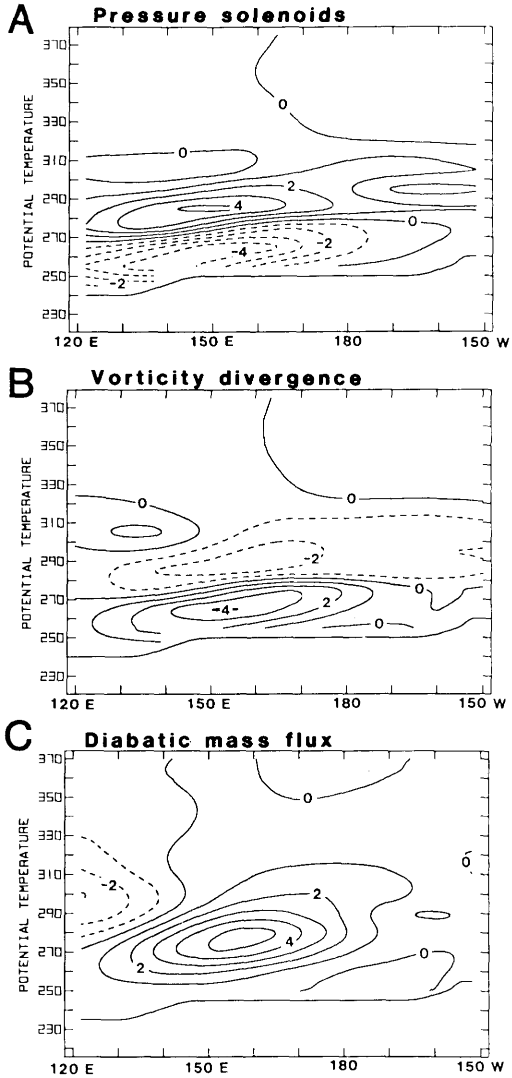

Fig. 10. Isentropic vertical cross sections of mean layer-integrated (A) mass-dry static energy solenoids and (B) vorticity divergence for 10 K isentropic layers and (C) vertical diabatic mass flux along the Pacific storm track for January 1979 (units (A) and (B), $10^{-7}\,\mathrm{kg\,m^{-2}\,s^{-2}}$, (C) $10^{-3}\,\mathrm{kg\,m^{-2}\,s^{-1}}$). The cross section along 43°N extends zonally from 120°E to 150°W.

angular momentum by pressure torques. Both processes involve a transfer of momentum by pressure stresses across inclined isentropic surfaces. In the case of dynamic vorticity, this transfer of momentum by solenoidal processes induces shear or curvature of the momentum field $\rho J_\theta U$. In the case of angular momentum, pressure torques induce a moment of momentum about an axis of rotation.

In a diagnostic study of the relation between the isentropic angular momentum balance and the isentropic dynamic vorticity balance of cyclones, Wash (1975) verified the correspondence of the two-layered structure of azimuthally averaged sources of storm angular momentum by pressure torques with the two-layered structure of areally averaged sources of dynamic vorticity by mass-dry static energy solenoids. During the mature phase of cyclone development, the azimuthally averaged pressure torque is negative at colder potential temperatures and positive at warmer potential temperatures (Johnson and Downey, 1976; Johnson and Hill, 1986). The storm angular momentum is transferred horizontally from colder to warmer air across the inclined isentropic surfaces within the baroclinic structure of storms (Johnson and Downey, 1976; Wash, 1975; Johnson and Hill, 1986). For the time-averaged dynamic vorticity balance, the transfer by mass-dry static energy solenoids along the storm tracks from the sink beneath 280 K to a source above, is manifested as a direct exchange of dynamic vorticity from continental polar to maritime polar or subtropical air masses. Implicitly this transfer of dynamic vorticity within regional circulations also represents a transfer of storm angular momentum in the same sense.

Within an isentropic perspective on forcing of cyclone development, the transfer of dynamic vorticity and angular momentum by pressure stresses from lower- to higher-valued isentropic layers contributes to the forcing of occlusion (Johnson and Downey, 1976; Johnson and Hill, 1987). Through this process colder air is forced into the vortex by negative solenoids in lower-valued isentropic layers and warmer air is forced out of the vortex by positive solenoids in higher-valued isentropic layers. This systematic solenoidal exchange of vorticity in relatively shallow baroclinic disturbances over the Kuroshio and Gulf Stream currents in the western ocean basins is fundamental to the vertical development and occlusion of vortices as they propagate toward the eastern ocean basins where the planetary-scale Aleutian and Icelandic lows reside. Thus, the large-scale zonal and meridional exchange of air masses in coupling heat sources and sinks in extratropical latitudes and the associated baroclinic redistribution of dynamic vorticity are fundamental to the maintenance of the semi-permanent features of the planetary circulation.

(b) *Vorticity divergence*

An outstanding feature of the Northern Hemisphere dynamic vorticity balance in the 280–290 K layer (Fig. 9b) is the sink by the vorticity divergence centered southwest of Iceland. Somewhat weaker sinks by divergence extend from the Mediterranean to the Caspian Sea and from Korea to the Gulf of Alaska. These three regions of vorticity divergence coincide with the primary storm tracks of the Atlantic, Mediterranean and Pacific, again indicating the importance of migratory disturbances in large-scale exchange. Flanking the mid-latitude regions of vorticity divergence are areas of vorticity convergence across northern portions of Europe and Asia, Canada and the subtropics. As in the 260–270 K layer, the mean divergence of absolute vorticity transport for the 280–290 K layer is determined largely by the divergent component associated with the geostrophic mode of mass divergence (Fig. 12c).

The mean coupling between vorticity exchange and differential heating is further illustrated in the monthly averaged cross section of Figs. 10 and 11. Along the East Asian/Pacific storm track, centers of maximum solenoidal source/sinks, vorticity divergence and upward diabatic mass flux coincide near approximately 150° E. Along the Atlantic storm track, two centers of maximum solenoidal source/sinks and vorticity divergence, one located downstream of the central United States coast near 35° N and the other located south of Iceland near 55° N, coincide with centers of upward diabatic mass flux in these regions. The diabatic mass flux in Figs. 10c and 11c has a maximum near 270 to 290 K that reflects a maximum in latent heat release in extratropical cyclones. A comparison of Figs. 10 and 11 reveals the correspondence of the zero isopleths of the 270–280 K solenoids and vorticity divergence with the relative maxima of diabatic mass flux. Beneath the level of maximum upward diabatic mass flux, the increase of dynamic vorticity through horizontal mass convergence and vortex stretching is coupled with the increase of the upward diabatic mass flux. Above this level, the decrease of dynamic vorticity through horizontal mass divergence and shrinking is coupled with the decrease of upward diabatic mass flux.

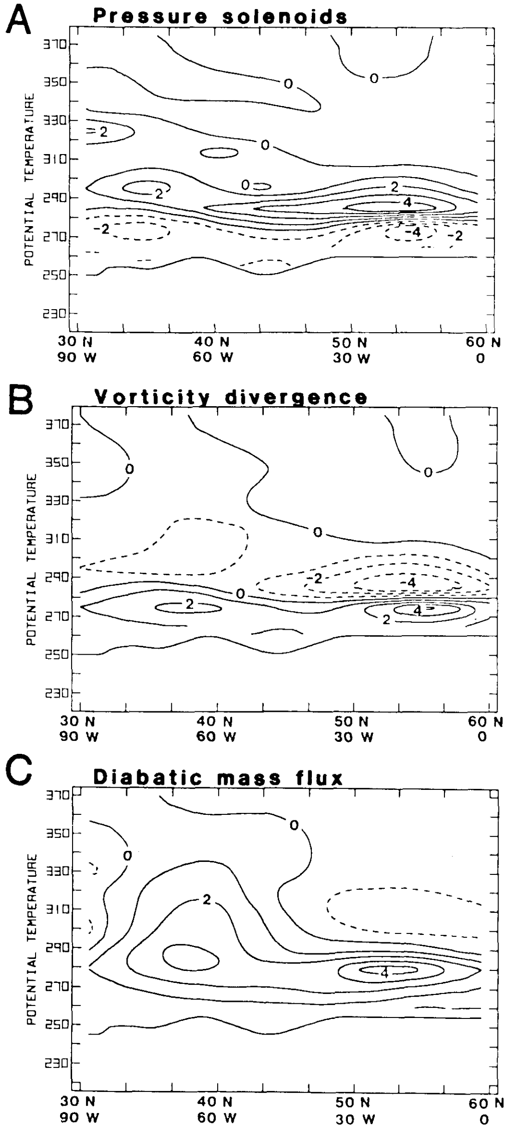

Fig. 11. Same as Fig. 10 except the cross section along Atlantic Ocean storm track extends from 30° N and 90° W to 60° N and 0°.

The distribution of the irrotational component of absolute vorticity transport for the 280–290 K layer (Fig. 9c) captures the systematic lateral transport of absolute vorticity from solenoidal

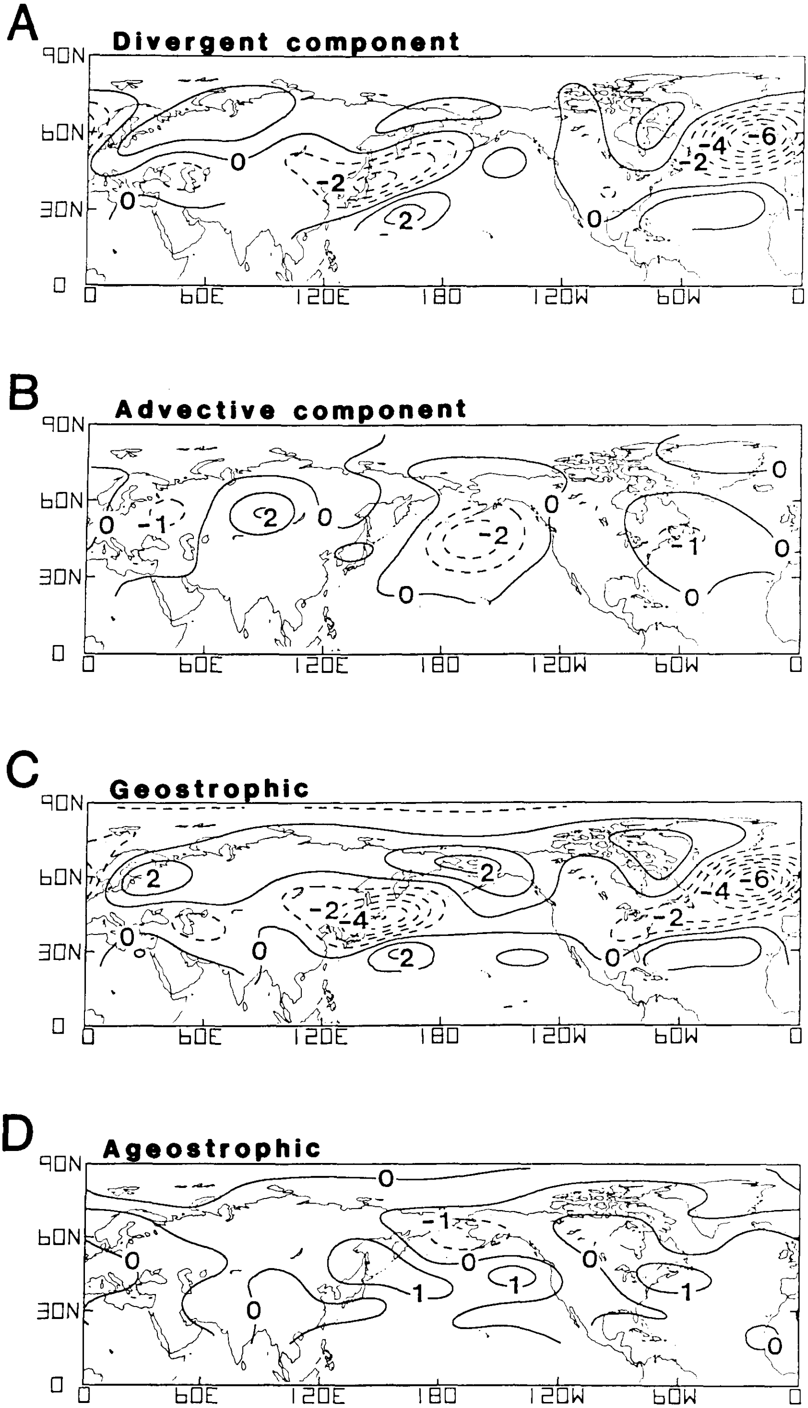

Fig. 12. Same as Fig. 8 except for the 280–290 K isentropic layer.

source regions across the Pacific and Atlantic to solenoidal sink regions across Asia, North America and the subtropical Pacific and Atlantic. The coupled nature of the irrotational modes of mass and absolute vorticity transport in this 280–290 K layer and the 260–270 K layer (compare Figs. 6c and 9c) confirm the importance of the quasi-horizontal transport of absolute vorticity within horizontal branches of isentropic mass circulation. As such, the diagnostic evidence verifies the importance of isentropic monsoonal circulations in determining a common scale between differential heating, the irrotational components of mass, energy and entropy transport, and the exchange of dynamic vorticity (Johnson and Hoerling, 1988; Johnson, 1989).

5. Summary and discussion

The wintertime exchange of dynamic vorticity in the underworld of the Northern Hemisphere has been studied through an isentropic analysis employing the ECMWF Level IIIb data. This exchange is linked directly with the distribution of heat sources and sinks in extratropical and polar latitudes and occurs through a distinct thermally direct isentropic mass circulation involving the migration of polar and arctic air masses in the underworld (Johnson, et al., 1985). This mass circulation leads to a systematic influence of dynamical processes occurring in migratory extratropical cyclones and anticyclones on the planetary circulation by effecting a net exchange of dynamic vorticity from quasi-stationary anticyclones over continents to cyclones over oceans. In the Northern Hemisphere, the predominantly zonal exchange between heat source and heat sink regions of middle and high latitudes beneath 300 K contrasts with the meridional exchange in isentropic layers upward to 400 K between the net heat sinks of polar latitudes and heat sources of tropical latitudes. The latter involves movement of polar air masses of the underworld equatorward and subtropical and tropical air masses in the overworld poleward. An analysis of dynamic vorticity balance throughout the troposphere with emphasis on the maintenance of polar and subtropical jet streams in relation to global monsoonal circulations appears in Hoerling (1987).

The balance of dynamic vorticity in the underworld ($\theta \leqslant 300$ K) is maintained by a horizontal transport of absolute vorticity from source regions by mass-dry static energy solenoids to corresponding sink regions. Beneath 280 K, positive solenoidal source regions occur in the mean anticyclones over northeastern Europe, northern Asia, Canada and much of Greenland, while negative solenoidal sink regions extend zonally from the eastern seaboards of Asia and North America to the north central Pacific and Atlantic Oceans. Thus, balance involves the net transport of absolute vorticity from the solenoidal sources of Asia, North America and Greenland to the solenoidal sinks of the Pacific and Atlantic Oceans, both of which are linked directly with the thermally forced isentropic mass circulation of the underworld. The absolute vorticity transport in the 280–300 K isentropic layers is likewise linked with the return branch of the thermally forced mass circulation and the poleward and eastward movement of maritime polar air masses.

The important role of solenoidal processes in the maintenance of the rotational component of the isentropic mass transport supports Bjerknes' (1937) concepts on the first-order effect of solenoidal processes in the general circulation and their relation to differential heating. Within the isentropic structure, differential heating and solenoidal processes are intrinsically coupled with the geostrophic nature of transport processes in latitudes where the effects of the earth's rotation are important (Johnson and Hoerling, 1988). In the underworld, the wintertime irrotational isentropic mass circulation is realized primarily as the exchange of continental and maritime polar air masses through which energy, entropy and vorticity are exchanged between heat source and sink regions. This systematic coupling of exchange processes with heat sources and sinks can only be established in a direct sense by isentropic analyses.

It is important to understand why a direct coupling between heat sources and sinks and vorticity can only be established through isentropic analysis of dynamic vorticity and not by isobaric analyses. The first-order balance of isentropic dynamic vorticity balance is maintained largely by a compensation between solenoids and stretching of vortex tubes due to the geostrophic mass convergence. In the time-averaged state, the geostrophic mass convergence is directly coupled with stretching of vortex tubes through vertical diabatic mass flux. Within isobaric analyses, the horizontal invariance of mass within hydrostatic isobaric layers leads to the equality of dynamic vorticity (per unit mass) and kinematic vorticity. The first order balance of isobaric kinematic vorticity involves vorticity advection, stretching by ageostrophic mass convergence and the curl of the friction force (Holopainen and Oort, 1981; Mullen, 1986). The scale of these processes corresponds with the scale of secondary circulations that are forced by mass-momentum adjustment. Since there is no solenoidal source, this order of balance in isobaric coordinates is equivalent to the second-order balance of dynamic vorticity in isentropic coordinates which is related to agesotrophic processes. Analogously, through the utilization of isentropic kinematic vorticity, Petterssen (1950) was unable to establish a direct link between vorticity exchange and heat sources and sinks from diagnostic evidence.

Petterssen (1950) argued, however, that the maintenance of such wintertime features as the Icelandic and Aleutian lows and the Siberian high are coupled through the transport of vorticity, and that this transport must be linked with the distribution of heat sources and sinks. The problem of the general circulation was expressed by Petterssen (1950) in the following manner: "Given the mean temperature of the atmosphere and the approximate location of the heat and cold sources, is it possible on dynamic and thermodynamic principles to account for the maintenance of the above mentioned semi-permanent pressure systems and the tendency of travelling cyclones and anticyclones to follow, in a statistical sense, the observed patterns?". The empirical results presented herein have addressed this classic problem of the general circulation.

Presented in Fig. 13 is Petterssen's (1950) idealized model of vorticity exchange in the lower troposphere during winter stemming from his investigations on the behaviour of cyclones and anticyclones. The major features depicted in middle latitudes are regions of vorticity transport associated with travelling cyclones/anticyclones across the North Pacific and the North Atlantic. The primary feature in polar latitudes is the vorticity source region of high pressure across the Arctic and its equatorward extension across North America and Asia.

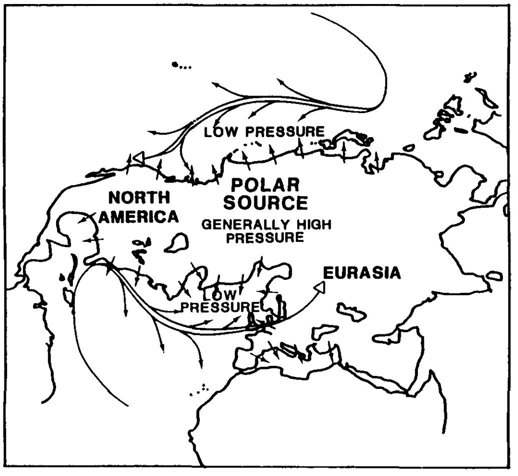

Fig. 13. A schematic representation (after Petterssen, 1950) of the wintertime transport of vorticity within the lower isentropic layers of the underworld from the source regions of anticylonic circulations over polar ice and land masses to the sink regions of cyclonic circulations over the North Atlantic and the North Pacific Oceans. As indicated by Petterssen (1950) the two elongated arrows represent the alternating influx of cyclonic and anticyclonic circulations. It is through this alternation that the transport of dynamic vorticity from continents to oceans is effected.

A transport of vorticity from heat sinks over continents to heat sources over oceans as envisaged by Petterssen is most apparent in the observed dynamic vorticity balance below the 280 K surface. This transport of vorticity from solenoidal sources over continents to solenoidal sinks over oceans by transient cyclonic/anticyclonic couplets corresponds with the paths of maximum alternation between cyclones and anticyclones as illustrated by the double shafted arrows across the Pacific and Atlantic Oceans in Fig. 13 (also see Fig. 13.8.2 in Petterssen, 1956). The sink regions of dynamic vorticity at the earth-atmospheric interface occur poleward and downstream of the oceanic storm tracks where the curl of the viscous stresses spins down the mean circulations of the Aleutian and Icelandic lows. The primary source regions of dynamic vorticity at the earth-atmosphere interface occur across the continents of middle and high latitudes where the curl of the pressure and viscous stresses combine to generate cyclonic dynamic vorticity within the large-scale anticyclonic circulations across northern Asia, North America and the Arctic. Through the diagnostic analysis of this study employing a global three-dimensional assimilated data set, the essential features of Petterssen's model relating vorticity exchange and differential heating in polar-extratropical latitudes has been established.

The present analysis reveals only a limited view of the forcing and maintenance of the general circulation that occurs in the underworld. The conditions in the overworld, the global scale of differential heating and the exchange of dynamic vorticity that occurs between the overworld and the underworld through baroclinic processes within the planetary-scale wave regime are considered in Hoerling (1987).

6. Acknowledgements

We wish to acknowledge the data on cyclone frequency for January 1979 provided by Linda (Whittaker) Keller for Fig. 2b and the assistance of Judy Mohr in typing the manuscript and Christine Johnson in drafting the figures. The comments and suggestions of Todd Schaack, Paul Spaete, Steve Silberberg and Russ Schneider were helpful in improving the manuscript. This research was supported by the National Science Foundation under Grants ATM-8602860 and ATM-8822427.

7. Appendix

List of symbols

$\boldsymbol{F}$	friction force
$\boldsymbol{U}$	horizontal velocity
J_θ	Jacobian for transformation of height to potential temperature $\lvert\partial z/\partial\theta\rvert$
f	Coriolis parameter
h	arbitrary function
k	kinetic energy
p	pressure
Q	curve of integration
z_θ	isentropic relative dynamic vorticity per unit mass
Z_θ	isentropic relative dynamic vorticity per unit volume $\mathrm{d}A\ \mathrm{d}\theta$
θ	potential temperature
δ	divergence of vector transport defined by eq. (8)
ρ	density
ζ_θ	isentropic relative kinematic vorticity
ψ	Montgomery stream function
X	transport potential function

Subscripts

ag	ageostrophic component
g	geostrophic component
ρ	mass transport

Operators

$(\bar{\phi})$	time average
∇_θ	quasi-horizontal operator in isentropic coordinates
∇_θ^2	quasi-horizontal laplacian operator in isentropic coordinates

REFERENCES

Bjerknes, V. 1937. Application of line integral theorems to the hydrodynamics of terrestrial and cosmic vortices. *Astrophys. Norv. 2*, 263–339.

Blackmon, M. L., Wallace, J. M., Lau, N.-C. and Mullen, S. L. 1977. An observational study of the Northern Hemisphere wintertime circulation. *J. Atmos. Sci. 23*, 1040–1053.

Chen, S.-C. and Trenberth, K. E. 1988. Forced planetary waves in the Northern Hemisphere winter: Wave-coupled orographic and thermal forcings. *J. Atmos. Sci. 45*, 682–703.

Derome, J. and Wiin Nielsen, A. 1971. The response of a middle latitude model atmosphere to forcing by topography and stationary heat sources. *Mon. Wea. Rev. 99*, 564–576.

Downey, W. K. and Johnson, D. R. 1978. The mass, absolute angular momentum and kinetic energy budgets of model-generated extratropical cyclones and anticyclones. *Mon. Wea. Rev. 106*, 469–481.

Gallimore, R. G. and Johnson, D. R. 1981. The forcing of the meridonal circulation of the isentropic zonally averaged circumpolar vortex. *J. Atmos. Sci. 38*, 583–599.

Held, I. 1983. Stationary and quasi-stationary eddies in the extratropical atmosphere: Theory. *Large-scale dynamical processes in the atmosphere*, (eds. R. P. Pearce and B. J. Hoskins). Academic Press. 127–168 pp.

Hoerling, M. P. 1987. *The global balance of dynamic vorticity in relation to heat sources and sinks.* Ph.D. thesis. University of Wisconsin-Madison, 246 pp.

Holopainen, E. O. and Oort, A. H. 1981. On the role of large-scale transient eddies in the maintenance of the vorticity and enstrophy of the time-mean atmospheric flow. *J. Atmos. Sci. 38*, 270–280.

Hoskins, B. J. and Karoly, D. 1981. The steady linear response of a spherical atmosphere to thermal and orographic forcing. *J. Atmos. Sci. 38*, 1179–1196.

Johnson, D. R. and Downey, W. K. 1976. The absolute angular momentum budget of an extratropical cyclone: Quasi-Lagrangian diagnostics 3. *Mon. Wea. Rev. 104*, 3–14.

Johnson, D. R. 1980. A generalized transport equation for use with meteorological coordinate systems. *Mon. Wea. Rev. 108*, 733–745.

Johnson, D. R. 1985a. *The global circulation during the FGGE year: On the balance of mass, energy, and angular momentum within isentropic and isobaric coordinates as revealed by different data sets.* WMO Proceedings of the Global Weather Experiment Seminar, 28–31 August 1984, Helsinki, Finland. GARP Special Report No. 42, II, 28–40.

Johnson, D. R. 1985b. *On the global distribution of heat sources and sinks and their relation to mass and energy transport.* WMO Report on the Seminar on Progress in Tropical Meteorology as a Result of the Global Weather Experiment, Tallahassee, Florida, 8–12 October 1984. GARP Special Report No. 44, III, 1–13.

Johnson, D. R., Townsend, R. D. and Wei, M.-Y. 1985. The thermally coupled response of the planetary-scale circulation to the global distribution of heat sources and sinks. *Tellus 37A*, 106–125.

Johnson, D. R. 1989. The forcing and maintenance of global monsoonal circulations: An isentropic analysis. In: *Advances in Geophysics.* (ed. B. Saltzman). Academic Press, vol. 31, pp. 43–316.

Johnson, D. R. and Hill, D. K. 1987. Quasi-Lagrangian diagnostics of a Mediterranean cyclone: Isentropic results. *Meteorology and Atmospheric Physics 36*, 118–140.

Johnson, D. R. and Hoerling, M. P. 1988. The definition and attributes of dynamic vorticity in isentropic analysis. *AMS Preprint Volume for the Palmén Symposium*, Helsinki, Finland, 28 August–2 September 1988, pp. 59–62.

Johnson, D. R., Yanai, M. and Schaack, T. K. 1987. Global and monsoonal distributions of atmospheric heat sources and sinks during the GWE. In: *Monsoon meteorology*, (eds. C.-P. Chang and T. N. Krishnamurti), Oxford University Press, 271–297.

Kao, S.-K. 1960. Transfer of momentum vorticity and the maintenance of zonal circulation in the atmosphere. *J. Meteor. 17*, 122–129.

Lau, N.-C. 1978. On the three-dimensional structure of the observed transient eddy statistics of the Northern Hemisphere wintertime circulation. *J. Atmos. Sci. 35*, 1900–1923.

Lau, N.-C. 1979a. The structure and energetics of transient disturbances in the Northern Hemisphere wintertime circulation. *J. Atmos. Sci. 36*, 982–995.

Lau, N.-C. 1979b. The observed structure of tropospheric stationary waves and the local balance of vorticity and heat. *J. Atmos. Sci. 36*, 996–1016.

Lenzen, A. J. 1980. *Diagnostic study of warm-core anticyclones associated with a blocking circulation pattern.* Ph.D. thesis, University of Wisconsin-Madison, 205 pp.

Palmén, E. 1951. The rôle of atmospheric disturbances in the general circulation. *Quart. J. R. Met. Soc. 77*, 337–354.

Palmén, E. and Alaka, M. A. 1952. On the budget of angular momentum in the zone between equator and 30° N. *Tellus 4*, 324–331.

Petterssen, S. 1950. Some aspects of the general circulation of the atmosphere. *Cent. Proc. R. Met. Soc.* 120–155.

Petterssen, S. 1956. *Weather analysis and forecasting*, 2nd ed., vol. I. McGraw-Hill, New York, 428 pp.

Schaack, T. K. 1982. *The global angular momentum balance for January 1979.* M.S. thesis, University of Wisconsin-Madison, 104 pp.

Schaack, T. K. and Johnson, D. R. 1989. *Atlas of the global distribution of heating during the GWE.* Space Science and Engineering Center, University of Wisconsin-Madison, Madison, Wisconsin, 150 pp.

Shaw, Sir Napier. 1930. *Manual of meteorology, the physical processes of weather, Vol. III.* Cambridge University Press, 445 pp.

Smagorinsky, J. 1953. The dynamical influence of large-scale heat sources and sinks on the quasi-stationary mean motions of the atmosphere. *Quart. J. R. Met. Soc. 79*, 342–366.

Swarztrauber, P. and Sweet, R. 1975. Efficient FORTRAN subprograms for the solution of elliptic partial differential equations. *NCAR Technical Note No. 109*, Atmospheric Technology Division, National Center for Atmospheric Research, Boulder, Colorado, 139 pp.

Townsend, R. D. and Johnson, D. R. 1985. A diagnostic study of the isentropic zonally-averaged mass circulation during the first GARP global experiment. *J. Atmos. Sci. 42*, 1565–1579.

Wash, C. H. 1975. *A momentum circulation budget for an extratropical cyclone.* M.S. thesis, University of Wisconsin-Madison, 113 pp.

Wei, M.-Y., Johnson, D. R. and Townsend, R. D. 1983. Seasonal distribution of diabatic heating during the first GARP global experiment. *Tellus 35*, 241–255.

Whittaker, L. M. and Horn, L. H. 1982. *Atlas of Northern Hemisphere extratropical cyclone activity, 1958–1977.* Department of Meteorology, University of Wisconsin-Madison, 67 pp.